SINGLE UNDERWATER IMAGE ENHANCEMENT USING DEPTH ESTIMATION BASED ON BLURRINESS

Yan-Tsung Peng, Xiangyun Zhao and Pamela C. Cosman

Department of Electrical and Computer Engineering,
University of California, San Diego,
La Jolla, CA 92093-0407.
Email: {yapeng, xiz019, pcosman}@ucsd.edu

ABSTRACT

In this paper, we propose to use image blurriness to estimate the depth map for underwater image enhancement. It is based on the observation that objects farther from the camera are more blurry for underwater images. Adopting image blurriness with the image formation model (IFM), we can estimate the distance between scene points and the camera and thereby recover and enhance underwater images. Experimental results on enhancing such images in different lighting conditions demonstrate the proposed method performs better than other IFM-based enhancement methods.

Index Terms— Underwater images, image enhancement and restoration, image blurriness, depth estimation.

1. INTRODUCTION

Underwater imaging suffers from visible degradation due to the propagated light attenuated with distance from the camera, primarily resulting from absorption and scattering effects. Thus, it has been a challenging task to restore and enhance underwater images because of the variation of physical properties involved for images taken in such environments. Underwater scenes are often low contrast with distant objects appearing misty and blurred.

Several attempts have been made to restore color, contrast and sharpness for such images using a simplified IFM [1] via depth estimation [2, 3, 4, 5, 6, 7] (DE). In [2, 4, 5], the scene depth is derived by the dark channel prior (DCP) [8], which was proposed to remove haze in natural terrestrial images by calculating the amount of spatially homogeneous haze using the darkest channel in the scene. It was observed that because points in the scene closer to the camera have a shorter path over which scattering occurs, dark pixels would remain dark as they would experience less brightening from scattered light. Thus, the DCP can be used to estimate the scene depth. Bianco et al. [3], instead of utilizing the DCP, adopted the maximum intensity prior (MIP) that uses the difference between the maximum intensity of the red channel and that of the green and blue channels to calculate the depth. In [6, 7], the underwater DCP was proposed, where only the blue and green channels are considered, since red light that possesses longer wavelength and lower frequency attenuates faster. However, these methods that only take RGB channels into account may lead to erroneous DE because the light absorption and different lighting conditions existing in underwater images make exceptions to those priors, which possibly results in poor image restoration.

In this paper, we take a different approach to estimate scene depth, which circumvents the aforementioned problem. Because larger scene depth causes more object blurriness for underwater images, we propose to measure the scene depth via image blurriness. Image blurriness measurement is often discussed in single image defocusing [9, 10]. In [9], a multi-scale edge detector is used to estimate pixel blurriness, and then the defocus map is generated by using the edge-aware interpolation method [11] in which the blurriness at non-edge pixels is interpolated and propagated by neighbouring edge pixels based on the similarities of luminance. In [10], the matting Laplacian [12] is applied to perform defocus map interpolation. However, the noise and low contrast may cause incorrect blurriness propagation, especially for underwater images. Moreover, these edge-aware interpolation methods entail high computation cost because they involve solving high-dimension linear equations. Therefore, we propose to use closing by morphological reconstruction [13] (CMR), which requires less computation cost and also decreases the chance of incorrect blurriness propagation. To this end, the estimated depth map by image blurriness is adopted in the IFM to restore and enhance underwater images for better visual quality in different lighting conditions.

The rest of the paper is organized as follows. In Section 2, we briefly review single image enhancement using DCP. The proposed method is described in Section 3. The experimental results are reported in Section 4. Finally, Section 5 summarizes the conclusions.

This work was supported in part by the National Science Foundation under Grant CCF-1160832.

2. SINGLE IMAGE ENHANCEMENT USING DARK CHANNEL PRIOR

The simplified IFM for underwater images is given as:

$$I(x) = J(x)t(x) + \beta(1 - t(x)), \tag{1}$$

where I is the observed intensity of the input image at pixel x, J is the scene radiance, β is the background light (BL), and t is the transmission medium map that describes the portion of the scene radiance that is not scattered or absorbed and reaches the camera. In this model, the transmission map is the depth map, i.e., smaller t means the scene point is farther from the camera.

In order to recover the scene radiance J, the DCP is proposed based on the statistics that about 75% of pixels in non-sky patches in outdoor images have zero values in the dark channel, which is written as Eq. (9) in [8] as:

$$\min_{y\in\Omega(x)} \left\{ \min_{c\in\{R,G,B\}} J^c(y) \right\} = 0, \tag{2}$$

where $\Omega(x)$ is a local patch centered at x, and J^c is the intensity of the scene radiance in channel c, where c is one of the R, G, B channels.

Applying the min operator to both sides of Eq. (1), the depth map is obtained [8] as:

$$t(x) = 1 - \min_{y\in\Omega(x)} \left\{ \min_{c\in\{R,G,B\}} \frac{I^c(y)}{\beta^c} \right\}. \tag{3}$$

Since the depth map has block-like artifacts, it can be refined by either image matting [12] or guided filtering [14].

Let the dark channel of the input image be $I_{dark}(x) = \min_{y\in\Omega(x)} \{\min_c I^c(y)\}$. To estimate the BL β, the top 0.1% brightest pixels in I_{dark} are picked and then the corresponding intensities in the input image are averaged, which tends to mean that the BL is getting estimated from the 0.1% farthest scene points in the image. Let $S_{0.1}$ be the set of the positions of those brightest pixels in I_{dark}. The estimated BL can be calculated as:

$$\beta^c = \frac{1}{|S_{0.1}|} \sum_{x\in S_{0.1}} I^c(x), \quad c \in \{r, g, b\}. \tag{4}$$

Finally, putting I, t and β into Eq. (1), the scene radiance J can be recovered as:

$$J(x) = \frac{I(x) - \beta}{\max(t(x), r_0)} + \beta, \tag{5}$$

where r_0 is typically set ranging from 0.3 to 0.5, empirically to increase the exposure of J for display.

As shown in Fig. 1, the method works in some cases. In Fig. 1(a), the rock in the foreground has very dark pixels which cause the dark channel to have a small value, so the rock is correctly estimated as being close. The background and farther objects have more scattering and lack very dark pixels, so the dark channel has a larger value, and these regions are correctly estimated to be far away. Fig. 1(b) is an example where the DCP does not work well, as the region on the abdomen of the devil ray is very bright and is mistakenly judged to be very far. Fig. 4 shows other examples where the DCP produces poor depth estimation.

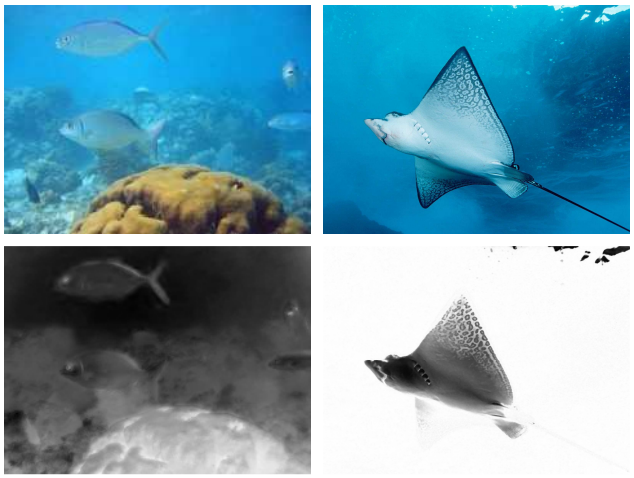

Fig. 1. Examples of depth estimation via the DCP for underwater images. (a) A successful case. (b) A failure case. (The original images come from [3] and www.webmastergrade.com for (a) and (b), respectively.)

3. PROPOSED DEPTH ESTIMATION AND ENHANCEMENT

To overcome the limitations inherent in the assumptions underlying the DCP approach, we propose DE based on blurriness. The proposed DE includes three steps:

1. Pixel blurriness estimation: calculate the difference between the original and the multi-scale Gaussian-filtered images to estimate the pixel blurriness map.

2. Rough depth map generation: apply the max filter to the pixel blurriness map by assuming the depth in a small local patch is uniform.

3. Depth map refinement: use CMR and the guided filter [14] to refine the depth map.

Let $G^{k,\sigma}$ be the input image filtered by a $k \times k$ spatial Gaussian filter with variance σ^2. The blurriness map B can be computed as:

$$B(x) = \frac{1}{n} \sum_{i=1}^{n} (|I(x) - G^{r_i, r_i}(x)|), \tag{6}$$

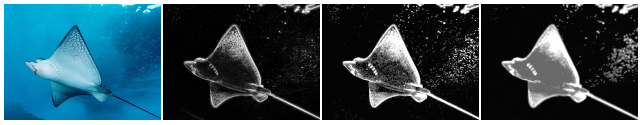

Fig. 2. (a) Original image. (b) Blurriness map from Eq. (6) (c) Rough depth map from Eq. (7). (d) Refined depth map.

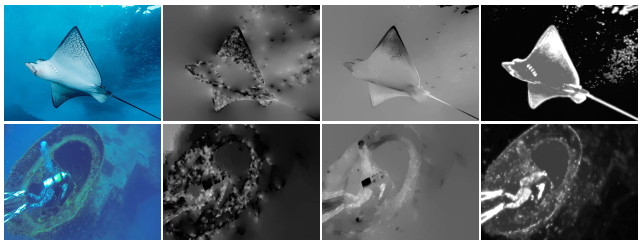

Fig. 3. Depth maps generated by different blurriness-based DE methods. (a) Original images. The depth maps obtained using the method in (b) [9], (c) [10], and (d) this paper.

where $r_i = 2^i n + 1$. Here, we assign $n = 4$. Next, we apply the max filter to B to calculate a rough depth map $\hat{t}$ as:

$$\hat{t}(x) = \max_{y \in \Omega(x)} B(y), \tag{7}$$

where $\Omega(x)$ is a $z \times z$ local patch centered at x. Here, we set $z = 7$. We then refine $\hat{t}$ by filling the holes caused by flat regions in the objects using CMR. Lastly, the guided filter is applied for smoothing to generate the refined depth map. Fig. 2 shows an example for the proposed DE. Additionally, the comparison of depth maps generated by different blurriness methods are shown in Fig. 3, where the proposed method produces better depth maps.

To use the depth map $\hat{t}$ in the IFM, $\hat{t}$ is stretched to a proper range $[r_0, r_1]$ as:

$$t(x) = \frac{\left[\hat{t}(x) - \min(\hat{t})\right](r_1 - r_0)}{\max(\hat{t}) - \min(\hat{t})} + r_0, \tag{8}$$

where r_1 is empirically set to 0.9, respectively. Additionally, we estimate the BL by t using the 0.1% farthest scene points according to the same process as in Section 2. Finally, we recover the scene radiance J using Eq. (5) with the t calculated in Eq. (8).

4. EXPERIMENTAL RESULTS

Previous methods for underwater image enhancement based on DE only used DCP- or MIP-based methods. In this section, we compare our blurriness-based DE against the DCP- and the MIP-based methods in an image enhancement context.

Table 1. The comparison of the BLs, $\beta = (red, green, blue)$, estimated by the compared enhancement methods.

Fig. 4	[3]	[4]	[6]	Proposed
Ex.1	$(2, 162, 240)$	$(202, 246, 252)$	$(7, 165, 238)$	$(4, 144, 211)$
Ex.2	$(15, 194, 216)$	$(248, 254, 254)$	$(105, 245, 242)$	$(0, 0, 0)$
Ex.3	$(9, 147, 251)$	$(204, 232, 233)$	$(37, 255, 207)$	$(23, 119, 194)$
Ex.4	$(15, 214, 243)$	$(206, 234, 243)$	$(4, 202, 228)$	$(1, 143, 195)$

In IFM-based image enhancement methods, there are two factors that strongly affect the enhancement results: the depth map and the BL estimation. Hence, the performance of the proposed method is evaluated by visual comparison with other IFM-based methods as well as the examination of the depth map and the BL. We use four underwater images captured in different lighting conditions for testing, shown in Fig. 4, where the depth maps all undergo simple individual contrast stretching or scaling steps for display in this paper. Table 1 lists the background lights of the four images estimated by the compared enhancement methods.

In Ex.1 of Fig. 4, all of the result images look properly enhanced only with a little color difference. Although the depth map and the BL are both inaccurately estimated by [4], its enhanced result is good only because of the extra color correction process in [4].

In Ex.2, the depth maps and the BL obtained by [3] and [6] are incorrect, which leads to even dimmer background scene. For [4], the background scene is wrongly regarded as being close to the camera, making no difference in the background after enhancement. In contrast, the proposed method using a better depth map and proper BL provides a more satisfactory enhancement result with a brighter and clearer background.

In Ex.3, the imprecise depth maps generated by [3], [4], and [6] cause color distortion in the output images while our method presents more natural color and better contrast.

In Ex.4, color distortion can be found in the output images obtained by [4] and [6] due to erroneous depth estimation while the result images yielded by [3] and the proposed method are enhanced with better global contrast.

5. CONCLUSION

In this paper, for underwater image enhancement, we have proposed to exploit image blurriness to measure the scene depth instead of using DCP. Combining image blurriness with IFM, we presented pleasing enhanced images. The depth estimation based on blurriness is shown to work well for a wide variety of images. The experimental results show that the proposed method can produce better enhanced underwater images in different lighting conditions compared to other IFM-based enhancement methods.

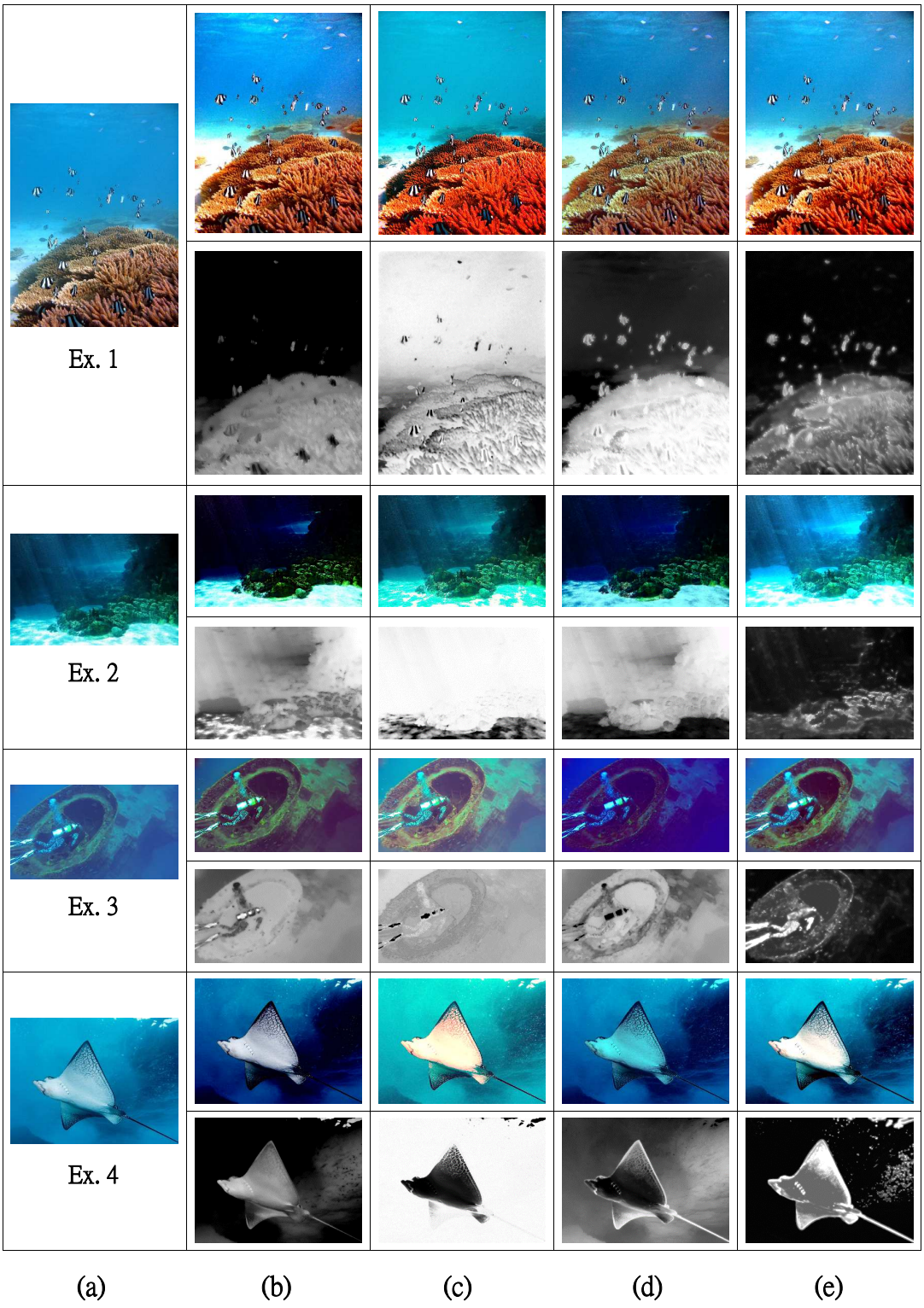

Fig. 4. Examples of the underwater image enhancement in different lighting conditions. (a) Original image. The enhanced images and the corresponding depth maps obtained using (b) [3], (c) [4], (d) [6], and (e) the proposed method. (The original image of Ex. 1 comes from [3]. For Ex. 2, the image is downloaded from della-stock.deviantart.com/art/Hercules-Looking-At-Megara-507373287, and credited to Daniella Koontz.)

6. REFERENCES

[1] R. Fattal, "Single image dehazing," ACM Transactions on Graphics, vol.27, no. 3, pp. 721-729, 2008.

[2] L. Chao and M. Wang, "Removal of water scattering," *in Proc. IEEE Int. Conf. Comput. Engin. and Tech. (ICCET)*, vol. 2, pp. 35-39, Apr. 2010.

[3] N. Carlevaris-Bianco, A. Mohan, and R. M. Eustice, "Initial results in underwater single image dehazing," *in Proc. IEEE Oceans*, pp. 1-8, 2010.

[4] H. Yang, P. Chen, C. Huang, Y. Zhuang and Y. Shiau, "Low complexity underwater image enhancement based on dark channel prior," *Int. Conf. Innov. in Bio-inspired Comput. and App. (IBICA)*, pp. 17-20, Dec. 2011. 17-20, 2011.

[5] J. Y. Chiang and Y.-C. Chen, "Underwater image enhancement by wavelength compensation and dehazing," *IEEE Trans. Image Process.*, vol. 21, pp. 1756-1769, Apr. 2012.

[6] H. Wen, Y. Tian, T. Huang, and W. Gao, "Single underwater image enhancement with a new optical model," *in Proc. IEEE Int. Symp. Circ. & Syst. (ISCAS)*, May 2013, pp. 753-756.

[7] P. Drews, E. do Nascimento, F. Moraes, S. Botelho, and M. Campos, "Transmission Estimation in Underwater Single Images," *in Proc. IEEE Int. Conf. Comput. Vis. Workshops (ICCVW)*, pp. 825-830, Dec. 2013.

[8] K. He, J. Sun, and X. Tang, "Single image haze removal using dark channel prior," *IEEE Trans. Pattern Anal. Mach. Intell.*, vol. 33, no. 12, pp. 2341-2353, Dec. 2011.

[9] S. Bae and F. Durand, "Defocus magnification," *in Proc. Comput. Graph. Forum.*, vol. 26, no. 3, pp. 571-579, 2007.

[10] S. Zhuo and T. Sim, "Defocus map estimation from a single image," *Pattern Recognit.*, vol. 44, no. 9, pp. 1852-1858, Sep. 2011.

[11] A. Levin, D. Lischinski, and Y. Weiss, "Colorization using optimization," ACM Trans. on Graphics 23(3), pp. 689-694, 2004.

[12] A. Levin, D. Lischinski, and Y. Weiss, "A Closed-Form Solution to Natural Image Matting," *IEEE Trans. Pattern Anal. Mach. Intell.*, vol. 30, no. 2, pp. 228 - 242, Feb. 2008.

[13] P. Soille, "Morphological Image Analysis: Principles and Applications," Springer-Verlag, 1999, pp. 173-174.

[14] K. He, J. Sun, and X. Tang, "Guided image filtering," *IEEE Trans. Pattern Anal. Mach. Intell.*, vol. 35, no. 6, pp. 1397-1409, Oct. 2012.